HRI-P-08-04-003
SISSA 27/2008/EP

Neutrino Oscillation Parameters After High Statistics KamLAND Results

Abhijit Bandyopadhyay[a], Sandhya Choubey[a], Srubabati Goswami[a], S.T. Petcov[b,c] [1], D.P. Roy[d,e]

[a)] *Harish-Chandra Research Institute, Chhatnag Road, Jhunsi, Allahabad 211 019, India,*
[b)] *Scuola Internazionale Superiore di Studi Avanzati, I-34014, Trieste, Italy,*
[c)] *INFN, Sezione di Trieste, Trieste, Italy,*
[d)] *AHEP Group, Instituto de Fisica Corpuscular (IFIC), CSIC-U. de Valencia, Edificio de Instituto de Paterna, Apartado de Correos 22085, E-46071 Valencia, Spain*
[e)] *Homi Bhabha Centre for Science Education, Tata Institute of Fundamental Research, Mumbai 400088, India*

Abstract

We do a re-analysis to asses the impact of the results of the Borexino experiment and the recent 2.8 KTy KamLAND data on the solar neutrino oscillation parameters. The current Borexino results are found to have no impact on the allowed solar neutrino parameter space. The new KamLAND data causes a significant reduction of the allowed range of Δm^2_{21}, determining it with an unprecedented precision of 8.3% at 3σ. The precision of Δm^2_{21} is controlled practically by the KamLAND data alone. Inclusion of new KamLAND results also improves the upper bound on $\sin^2\theta_{12}$, but the precision of this parameter continues to be controlled by the solar data. The third mixing angle is constrained to be $\sin^2\theta_{13} < 0.063$ at 3σ from a combined fit to the solar, KamLAND, atmospheric and CHOOZ results. We also address the issue of how much further reduction of allowed range of Δm^2_{21} and $\sin^2\theta_{12}$ is possible with increased statistics from KamLAND. We find that there is a sharp reduction of the 3σ "spread" with enhanced statistics till about 10 KTy after which the spread tends to flatten out reaching to less than 4% with 15 KTy data. For $\sin^2\theta_{12}$ however, the spread is more than 25% even after 20 KTy exposure and assuming $\theta_{12} < \pi/4$, as dictated by the solar data. We show that with a KamLAND like reactor "SPMIN" experiment at a distance of ~ 60 km, the spread of $\sin^2\theta_{12}$ could be reduced to about 5% at 3σ level while Δm^2_{21} could be determined to within 4%, with just 3 KTy exposure.

[1] Also at: INRNE, Bulgarian Academy of Sciences, Sofia, Bulgaria

1 Introduction

Over the past few years there has been a paradigm shift in the studies of neutrino physics. The aim of neutrino experiments shifted from establishing the existence of neutrino mass and mixing to precision determination of these oscillation parameters. In the case of solar neutrino oscillation, this has been possible thanks to a succession of precision data from the SNO and KamLAND experiments over the past few years. First, the simultaneous measurement of solar neutrino events from both charged and neutral current interactions by the SNO experiment [1, 2] was instrumental in narrowing down the solar neutrino mass and mixing parameters to the region of the so called Large Mixing Angle (LMA) solution [3, 4, 5, 6]. This was confirmed by the KamLAND reactor (anti)neutrino experiment [7]. Moreover, it pinned down the solar neutrino mass parameter to two narrow bands called low-LMA and high-LMA (also called LMA-I and II, respectively), corresponding to the 1st and 2nd oscillation nodes [7, 8, 9]. Then came the data from the second phase (salt phase) of SNO, which had a better detection efficiency for the neutral current events [10]. Including this data in a global analysis constrained the range of the solar neutrino mixing angle further, ruling out maximal mixing at more than 6σ level [11, 12]. Besides, it strongly favoured the low-LMA region of solar neutrino mass over the high-LMA, allowing the latter only at the 3σ level. This was followed by the 766 Ty KamLAND data [13], which had a nearly 5 times higher statistics than their first data. Including this data set in a global analysis pinned down the solar neutrino mass finally to the low-LMA region, while ruling out high-LMA at more than 4σ level [14, 15, 16]. In particular, our two-flavour neutrino oscillation analysis determined the best-fit solar neutrino mass and mixing parameters to be $\Delta m^2_{21} = 8 \times 10^{-5} eV^2$ and $\sin^2\theta_{12} = 0.28$, with a 3σ spread of about 15% and 30% respectively [14]. Extending this analysis to the three-flavour neutrino oscillation we found these mass and mixing angle values to be robust. Finally, the three-flavour oscillation analysis led to a moderate improvement of the CHOOZ [17] limit on the third mixing angle, $\sin^2\theta_{13}$. It should be noted here that the most precisely determined neutrino parameter to date is the above mass parameter Δm^2_{21}; and the results from the KamLAND reactor neutrino experiment has played a pivotal role in this.

Recently the KamLAND experiment has published their 2.8 KTy data [18], which increases the statistics of their earlier data by almost 4 times. Besides, they have reduced their systematic error and expanded the analysis to include the visible energy range below 2.6 MeV. In this work we have updated our global analysis [14, 15, 19, 20] with the inclusion of this new KamLAND data. As we shall see, its most important effect is a further reduction of the 3σ spread of Δm^2_{21} by a factor of 2. We have also studied the effect of the first Borexino data [21] on the result of this global analysis.

Section 2 is devoted to a two-flavour neutrino oscillation analysis of the global solar neutrino data along with the new KamLAND reactor neutrino data. In Section 3 we extend this to a three-flavour neutrino oscillation analysis to check the robustness of the oscillation parameters and also to update the limit on the third mixing angle. In section 4 we study the impact of future data from Borexino and KamLAND experiments on the precision of the solar neutrino mass and mixing angle. We also discuss how the precision of this mixing angle measurement can be improved dramatically by running a KamLAND type reactor SPMIN neutrino experiment at a lower baseline length of 60 km [22]. We conclude by summarizing our main results in section 5.

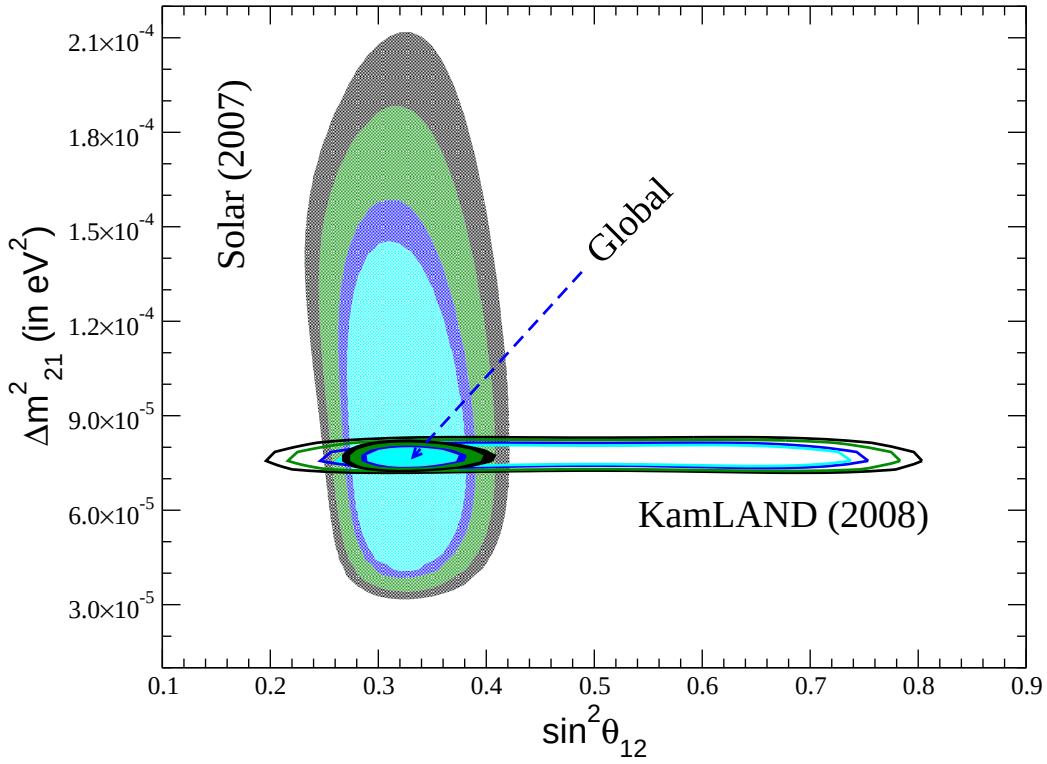

Figure 1: The 90%, 95%, 99% and 99.73% C.L. allowed regions in the Δm^2_{21} $-\sin^2\theta_{12}$ plane, obtained in a combined χ^2-analysis of the global solar neutrino and the 2.8 KTy KamLAND spectrum data (shaded areas). The regions allowed by the solar neutrino data and 2.8 KTy KamLAND data are also shown separately.

2 Two Flavour Neutrino Oscillation Analysis

We begin by reporting the status of the solar neutrino oscillation parameters Δm^2_{21} and $\sin^2\theta_{12}$. We present the allowed regions in the $\Delta m^2_{21} - \sin^2\theta_{12}$ plane and investigate the impact of the new sets of results, *viz.*, the effect of adding the Borexino data, and the impact of the high statistics KamLAND results.

2.1 Oscillation Parameters from Solar Neutrino Data

The first results from Borexino experiment were announced last year [21] providing the first real time measurement of sub-MeV solar neutrinos. The observed rate is $47 \pm 7(stat) \pm 12(syst)$ /(day.100 ton) whereas the expected rate without oscillation is 75 ± 4/(day.100ton) according to the Standard Solar Model of [23].

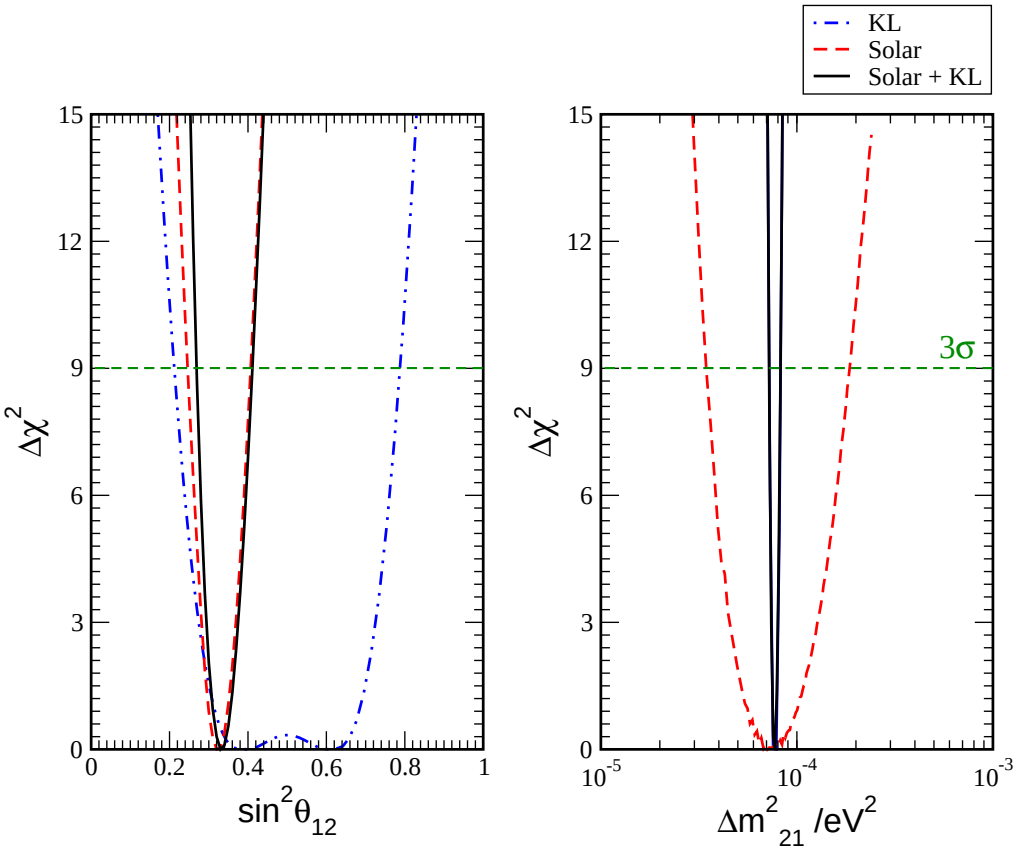

Figure 2: The $\Delta\chi^2$ as a function of Δm^2_{21} (right panel) and $\sin^2\theta_{12}$ (left panel). The results shown in both panels are obtained by allowing all the other parameters to vary freely. The dashed line shows the 3σ limit corresponding to 1 parameter fit. The lines for only KL and solar+KL are indistinguishable in the right panel.

This corresponds to an observed to expected Borexino rate of $R_B = 0.62 \pm 0.18$. We include this datum in our solar neutrino analysis and find the 90%, 95%, 99% and 99.73% allowed regions in the Δm^2_{21} $-\sin^2\theta_{12}$ parameter space. These are shown as hatched contours in Fig. 1. We have used in this analysis the solar neutrino data on the total event rates from the radiochemical experiments, Chlorine (Homestake) [24] and Gallium (Gallex, SAGE and GNO combined) [25], the 1496 day 44 bin Zenith angle spectrum data from SuperKamiokande [26], and data from phase I (pure D_2O phase) [2] and phase II (salt phase) [10, 27] of the SNO experiment. For the SNO data set, we include the combined Charged Current (CC), Neutral Current (NC) and Electron Scattering (ES) 34 bin energy spectrum data from phase I and the 34 bin CC energy spectrum data (17 day bins and 17 night bins), day and night NC rate data and day and night ES rate data from the phase II. The ^8B flux normalization factor f_B is left to vary freely in the analysis. For the other solar neutrino fluxes (pp, pep, ^7Be, CNO, hep), the predictions and estimated uncertainties from standard solar model (SSM) [23] (BP04) have been utilized. For further details of our solar

neutrino code and error analysis we refer the reader to our earlier papers [3, 4, 11].

We find that the present Borexino results make no impact on the allowed regions in the solar neutrino oscillation parameter space. The best-fit point from global solar neutrino data analysis stays unchanged at [19, 20]

$$\Delta m^2_{21} = 6.4 \times 10^{-5}\ \mathrm{eV}^2, \quad \sin^2\theta_{12} = 0.33, \quad f_B = \ 0.84. \tag{1}$$

These values of Δm^2_{21} and $\sin^2\theta_{12}$ imply adiabatic MSW [28] conversions of the higher energy ^8B neutrinos contributing to the SNO CC and SK event rates. The corresponding solar ν_e survival probability is given by $P_{ee} \simeq \sin^2\theta_{12}$. For the low energy pp neutrinos, which give the dominant contribution to the signal in the Ga-Ge experiments (SAGE, GALLEX/GNO), the predicted ν_e survival probability is $P_{ee} = 1 - 0.5\sin^2 2\theta_{12}$. Using the indicated expressions for P_{ee}, one can roughly check that the best-fit parameters given in Eq. (1) provide an excellent fit to the global solar neutrino data. From an exact numerical analysis we obtain with a $\chi^2 = 114$ for 119 degrees of freedom.

To quantify the constraint the global solar neutrino data imposes on the parameters Δm^2_{21} and $\sin^2\theta_{12}$ individually, we show the $\Delta\chi^2$ as a function of these parameters in the right and left panels of Fig. 2. Parameters which do not appear on the x-axis are left to vary freely in the fit. The red dashed lines correspond to the case where only solar neutrino results are included. The constraints on the individual oscillation parameters at any given C.L. for a one parameter fit can be read off from this figure. We give in the first row of Table 1 the ranges corresponding to the 3σ C.L. We also tabulate the corresponding "spread" which quantifies the uncertainty on the given oscillation parameter and is defined as

$$\mathrm{spread} = \frac{prm_{max} - prm_{min}}{prm_{max} + prm_{min}} \times 100, \tag{2}$$

where prm denotes the parameter Δm^2_{21} or $\sin^2\theta_{12}$, and prm_{max} and prm_{min} are the maximal and minimal values of the chosen parameter allowed at a given C.L. Solar neutrino results restrict $\sin^2\theta_{12}$ to be uncertain at 3σ by only $\pm 30\%$ around the best-fit, while for Δm^2_{21} the 3σ uncertainty is still as large as $\pm 70\%$.

2.2 Neutrino Oscillation Parameters from KamLAND Data Alone

In their most recent paper, the KamLAND collaboration has made public, data corresponding to a statistics 2.8 KTy [18]. The earlier data releases were for 0.162 KTy [7] and 0.7663 KTy [13]. Apart from an increased exposure time, the new data set is based on enlarged fiducial volume, full volume calibration to reduce the systematic error and expansion of the analysis to include the visible energy [2] spectrum below 2.6 MeV. All these have been very important improvements, especially the measurement of the spectrum below 2.6 MeV. The earlier two data sets from KamLAND were only for visible energy above 2.6 MeV, while the latest data set covers the entire available reactor spectrum, with threshold visible energy of 0.9 MeV. We use the 13 bin KamLAND spectrum data

[2]The visible energy is defined as $E_{vis} \simeq E_\nu - 0.8$ (MeV), where E_ν is the energy of the antineutrino.

Data set used	(3σ)Range of Δm^2_{21} eV^2	(3σ)spread in Δm^2_{21}	(3σ) Range of $\sin^2\theta_{12}$	(3σ) spread in $\sin^2\theta_{12}$
only sol	3.0 - 17.0	70%	$0.21 - 0.39$	30%
sol+162 Ty KL	4.9 - 10.7	37%	$0.21 - 0.39$	30%
sol+ 766.3 Ty KL	7.2 - 9.5	14%	$0.21 - 0.37$	27%
sol+2.8 KTy KL	$7.1 - 8.3$	7.8%	0.26 - 0.42	23.5%
only KL	*7.2 − 8.5*	*8.3%*	*0.2 - 0.5*	*43%*

Table 1: 3σ allowed ranges of Δm^2_{21} and $\sin^2\theta_{12}$ from the analysis of the global solar neutrino, and global solar neutrino + KamLAND (past and present) data. We show also the % spread in the allowed values of the two neutrino oscillation parameters. Note that for only KamLAND we ignore the allowed region of $\sin^2\theta_{12}$ in the Dark Zone ($\theta_{12} > \pi/4$) so that the maximum allowed value of $\sin^2\theta_{12}$ is 0.5

with a threshold from 0.9 MeV and define a χ^2 assuming a Gaussian distribution as

$$\chi^2_{\rm KL} = \sum_{i,j=1}^{N} (R_i^{\rm expt} - R_i^{\rm theory})(\sigma^2_{ij})^{-1}(R_j^{\rm expt} - R_j^{\rm theory}) \tag{3}$$

where $R^{\rm theory}$ and $R_i^{\rm expt}$ are the theoretically predicted and experimentally observed number of events in the i^{th} energy bin, and σ^2_{ij} is the error correlation matrix comprising of the statistical and systematic errors. The latter is taken to be 4.1%, fully correlated between the energy bins. The other details of our analysis can be found in [8, 14, 29]. Some of the reactors, particularly the Kashiwazaki-Kariwa and Fukushima I and II reactor complexes, were partially/totally shut-down during some of the period of data taking in KamLAND. We have approximately taken into account this change in the flux due to the reactor shut-down using the plots showing the time variations of the number of fissions in a given reactor and hence the expected reactor $\bar{\nu}_e$ flux in KamLAND [30]. We have also used the information on the reactor operation schedules available on the web [31].

The 90%, 95%, 99% and 99.73% C.L. allowed areas in the $\Delta m^2_{21} - \sin^2\theta_{12}$ parameter space, obtained using only the KamLAND data, can be seen within the open contours in Fig. 1. We show the allowed regions derived from the solar neutrino and KamLAND data taken individually in the same plot to allow for better comparison. The best-fit point for the KamLAND data alone, according to our analysis, is at

$$\Delta m^2_{21} = 7.7 \times 10^{-5}\ {\rm eV}^2, \quad \sin^2\theta_{12} = 0.39\ . \tag{4}$$

We note that both these best-fit values are larger than those obtained from the analysis of the solar neutrino data only. Note also that while the KamLAND data constrains Δm^2_{21} much better than the solar neutrino data, the constraint on the mixing parameter $\sin^2\theta_{12}$ from the solar neutrino data is much stronger. The range of allowed values for Δm^2_{21} and $\sin^2\theta_{12}$ at a given C.L. derived using the KamLAND data alone can be seen from the blue dashed lines in Fig. 2. The limits at 3σ

and the corresponding spread are given in Table 1. The latest KamLAND data alone excludes the high-LMA solution at more than 4σ. Note that the earlier 766 Ty KamLAND results disfavored high-LMA at 2.56σ only (1 parameter fit).

2.3 Constraints from Combined Solar and KamLAND Data Analysis

For the combined analysis of solar and KamLAND data we define the global χ^2 as

$$\chi^2_{global} = \chi^2_{\odot} + \chi^2_{KL} \ , \tag{5}$$

where χ^2_{KL} is the χ^2 for the KamLAND analysis given in Eq. (3), and $\chi^2_{\odot}$ is the χ^2 computed from the global analysis of the world solar neutrino data. We refer the reader to our earlier papers [3, 4, 11] for the details concerning $\chi^2_{\odot}$. The results are plotted as C.L. contours shown by the shaded zones in Fig. 1. We find that with the inclusion of the latest KamLAND spectrum data, the allowed range of Δm^2_{21} is sharpened considerably and the solar neutrino data plays practically no role in constraining Δm^2_{21}. On the other hand, the solar neutrino data is instrumental in reducing the allowed range of values of $\sin^2\theta_{12}$. The best-fit for combined solar neutrino and KamLAND data analysis is at,

$$\Delta m^2_{21} = 7.7 \times 10^{-5}\ \mathrm{eV}^2, \quad \sin^2\theta_{12} = 0.33, \quad f_B = 0.84. \tag{6}$$

The best-fit value of Δm^2_{21} we find agrees very well with that obtained by the KamLAND collaboration [18], while our best fit value of $\sin^2\theta_{12}$ is somewhat lower than that found in [18] because of differences in the fitting procedure. The best-fit value of Δm^2_{21} in the global fit is controlled by the KamLAND data, whereas the best-fit value of $\sin^2\theta_{12}$ is controlled by the global solar neutrino data. For similar recent analyses see also [32].

The individual constraints on Δm^2_{21} and $\sin^2\theta_{12}$ from the combined analysis of the solar neutrino and KamLAND data can be seen in Fig. 2, where we have plotted the $\chi^2 - \chi^2_{min}$ as a function of these parameters, taken one at a time. The corresponding 3σ allowed ranges and spread are given in Table 1. In order to show how the statistics from the KamLAND experiment has effected the precision of the measurement of Δm^2_{21} and $\sin^2\theta_{12}$, we have also given in the Table the 3σ allowed ranges and spread we had obtained by combining the solar neutrino data with the first KamLAND results (0.162 KTy data) and second KamLAND results (0.7663 KTy data). We can see that while the error on Δm^2_{21} has been dramatically reduced as KamLAND has accumulated more and more statistics, the uncertainty on $\sin^2\theta_{12}$ has remained rather large. The reason why KamLAND has limited ability in constraining $\sin^2\theta_{12}$ while its sensitivity to Δm^2_{21} is quite remarkable was pointed out in [22] and discussed in detail in [33, 34, 35, 36].

3 Three Neutrino Oscillation Analysis

So far we have restricted ourselves to two-generation oscillations where we have put the third mixing $\theta_{13} = 0$. However, oscillation of solar and KamLAND (anti)neutrinos do depend on θ_{13},

albeit weakly. Since $\Delta m^2_{31} \gg \Delta m^2_{21}$, the three-neutrino oscillation survival probability relevant for both solar and KamLAND (anti)neutrinos is approximately given by

$$P^{3g}_{ee} \simeq \cos^4\theta_{13}\, P^{2g}_{ee} + \sin^4\theta_{13}\ , \tag{7}$$

where P^{2g}_{ee} is ν_e survival probability in the case of two-neutrino oscillations. For solar neutrinos, P^{2g}_{ee} is given by the standard expression (see [37]), in which the electron number density N_e is replaced by [38] $N_e \cos^2\theta_{13}$. For KamLAND, P^{2g}_{ee} coincides with the usual two-neutrino vacuum oscillation probability used in the previous section. Thus, both solar and KamLAND have some sensitivity to θ_{13} and can therefore constrain it. We show in Fig. 3 the χ^2 obtained as a function of $\sin^2\theta_{13}$ when all other oscillation parameters are allowed to vary freely. While Δm^2_{21} and $\sin^2\theta_{12}$ are allowed to take any value in fit, the values of Δm^2_{31} are restricted within its current 3σ range. We show results for analysis of the CHOOZ reactor antineutrino and atmospheric results (solid line), as well as by adding solar and KamLAND data to this set (dashed line). The combined global data from solar neutrino, atmospheric neutrino and reactor antineutrino experiments put a bound of $\sin^2\theta_{13} < 0.063$ at 3σ. We have checked that there is practically no increase in the allowed regions in the $\Delta m^2_{21} - \sin^2\theta_{12}$ plane, when one goes from two to three flavor neutrino oscillation analysis of the global solar neutrino and KamLAND spectrum data. To show the impact of the solar and KamLAND data on three neutrino parameters we present in Fig. 4 the 90%, 95%, 99% and 99.73% C.L. allowed contours in the $\sin^2\theta_{12} - \sin^2\theta_{13}$ plane obtained from the combined analysis of the global solar neutrino data, the latest KamLAND data and CHOOZ data. It is to be noted that the P^{2g}_{ee} for high energy ^8B neutrinos is $\sim f_B \sin^2\theta_{12}$ while for KamLAND it is given as $1 - \sin^2 2\theta_{12} \sin^2 \Delta m^2_{21} L/4E$. Thus while for solar neutrinos an increase in θ_{13} implies an increase in θ_{12}, for KamLAND an increase in θ_{13} would imply a decrease in θ_{12} [39]. This opposing trend is instrumental in putting constraints in the $\sin^2\theta_{12} - \sin^2\theta_{13}$ plane.

4 What lies in the Future

The field of solar neutrino research has become quite mature now. The latest results from Borexino experiment has made real time detection of the ^7Be solar neutrinos possible and the results are consistent with the expectations from the LMA solution. The results from the KamLAND reactor data have provided independent and solid support to the LMA solution of the solar neutrino problem. With the recent KamLAND data, the precision of Δm^2_{21} gets controlled solely by KamLAND. At this point we ask the question, what will be the impact of future results from Borexino and KamLAND. In particular, we address two questions:

- Can improved precision of Borexino data play any role in further reducing the allowed ranges of Δm^2_{21} and/or θ_{12}?
- What will be the impact of a further increase of statistics of the KamLAND data?

To address the first point we analyze the solar neutrino data taking the Borexino rate as its present experimental value, but reducing the 1 sigma error (combined statistical and systematic) from 30 to 15%. However, even then there is no impact of Borexino on the allowed solar neutrino

parameter space. To asses the impact of the central value of the Borexino rate on the above result, we vary the allowed parameters in the combined solar and KamLAND analysis within their 3σ range and use the maximum and minimum predictions for the Borexino rate as the central value and accomplish an analysis of the combined solar data using 15% total error. But the allowed parameter space in the $\Delta m^2_{21} - \sin^2\theta_{12}$ plane remains stable against these variations. However, the measurement of the ^{7}Be neutrino flux with a higher precision will be very important for the determination of some of the basic solar model parameters [40].

In order to address the second question, we show in upper panels of Fig. 5 the spread in $\sin^2\theta_{12}$ (left panel) and Δm^2_{21} (right panel) as a function of the number of KTy of data in KamLAND. The x-axis starts from the current KamLAND statistics of 2.8 KTy. Note that while plotting the spread of $\sin^2\theta_{12}$, we ignore the allowed range of $\sin^2\theta_{12}$ in the dark zone ($\theta_{12} > \pi/4$), as dictated by the solar data. The figure shows that the spread in Δm^2_{21} shows a steady decrease till about 10 KTy of statistics of KamLAND after which the spread starts to decrease more gradually reaching to less than 4% with 15 KTy of statistics. The figure reveals that the spread in $\sin^2\theta_{12}$ from KamLAND also reduces with statistics, but even with 20 KTy of data, the spread in $\sin^2\theta_{12}$ is more than 25%, which is not significantly better than the value of 30% obtained from the current solar data (cf. Table 1). It has been already pointed out in the literature that maximum precision in $\sin^2\theta_{12}$ can be obtained in a reactor antineutrino experiment, identical to KamLAND in all respects, except that the baseline of this experiment would be tuned to the Survival Probability MINimum (SPMIN) [22, 35, 36]. Note that the present KamLAND experiment is situated at an average distance of about 180 km, which is a maxima of the survival probability (SPMAX). In the lower panels of this figure we show the projected sensitivity to these parameters in a "SPMIN" experiment [22, 35, 36]. For the current best-fit Δm^2_{21}, the baseline corresponding to SPMIN would be at about $L = 60$ km. One can see from the figure the remarkable sensitivity that this experiment would have to the mixing angle $\sin^2\theta_{12}$. Even with 1 KTy of data, we could determine $\sin^2\theta_{12}$ to $\pm 8\%$ precision and this could improve to about 5% with about 3 KTy of statistics. The sensitivity to Δm^2_{21} is also seen to be good. Although the survival probability is larger at the SPMAX than at the SPMIN, the latter is situated at a shorter distance of 60 km as compared to SPMAX (180 km at the present best fit value). So the distance factor makes up for the probability. Also it is to be noted that since KamLAND receives flux from several reactors at different distances, it is actually at an average SPMAX and so it cannot see the full distortion of the spectral shape. For the above reasons a dedicated SPMIN experiment also gives a comparatively better sensitivity to Δm^2_{21}. We could determine Δm^2_{21} within $\pm 4\%$ precision with 3 KTy data. The above results are obtained by taking $\sin^2\theta_{13} = 0$. However, inclusion of a non-zero $\sin^2\theta_{13}$ is not expected to alter the conclusions significantly [35]. Another experimental idea which could be used to return very good precision to the solar neutrino oscillation parameters consists of doping the SuperKamiokande with gadolinium [34, 41].

5 Conclusions

We have updated the solar neutrino parameter space including the Borexino results and the 2.8 KTy KamLAND spectrum data in global solar neutrino oscillation analysis.

The present Borexino results are found to have no impact on the solar neutrino parameter space. We also find that the allowed area in $\Delta m^2_{21} - \sin^2\theta_{12}$ plane remains stable against reduction in Borexino error by half its present value or by shifting the central value within the predicted 3σ range of the global solar and KamLAND analysis. The inclusion of the latest KamLAND results on the other hand causes a reduction in the spread in Δm^2_{21} by a factor of 2.

The allowed range of Δm^2_{21} is controlled practically by the KamLAND data. There is also a slight increase in the lower bound of θ_{12} with the inclusion of KamLAND data, though the precision in $\sin^2\theta_{12}$ is controlled by the solar data.

The 3σ upper limit on $\sin^2\theta_{13}$ from global solar, atmospheric and reactor antineutrino data is 0.063. There is practically no change in the allowed region in the $\Delta m^2_{21} - \sin^2\theta_{12}$ plane when one goes from two to three flavor neutrino oscillation analysis of the global solar neutrino and KamLAND spectrum data. The effect of combined solar and reactor antineutrino data on three flavour parameters have been presented in terms of allowed regions in the $\sin^2\theta_{12} - \sin^2\theta_{13}$ plane.

We also studied the impact of further reduction of KamLAND statistics on the precision of Δm^2_{21} and $\sin^2\theta_{12}$ and find that till about 10 KTy of statistics there is steady improvement of precision beyond which the spread in Δm^2_{21} flattens out, reaching less than 4% with 15 KTy of statistics. Spread in $\sin^2\theta_{12}$ shows hardly much improvement with increased KamLAND statistics. Even after accumulation of 20 KTy of statistics, the spread hovers around 25%, which is not much better than the 30% precision which the current solar data gives. A dramatic improvement in precision in $\sin^2\theta_{12}$ is possible in a dedicated KamLAND type of experiment at a distance of 60 km. Such an experiment can give 5% precision in $\sin^2\theta_{12}$ and 4% precision in Δm^2_{21} with only 3 KTy of statistics.

The work of A.B., S.C. and S.G. was supported by the Neutrino Project under the XIth plan at Harish Chandra Research Institute. D.P.R was supported in part by BRNS(DAE) through Raja Ramanna Fellowship and in part by MEC grants FPA2005-01269, SAB2005-0131. The work of S.T.P. was supported in part by the Italian INFN and MIUR programs "Fisica Astroparticellare" and "Fundamental Constituents of the Universe", and by the European Network of Theoretical Astroparticle Physics ILIAS/N6 (contract RII3-CT-2004-506222).

References

[1] Q. R. Ahmad *et al.* [SNO Collaboration], Phys. Rev. Lett. **87**, 071301 (2001).

[2] Q. R. Ahmad *et al.* [SNO Collaboration], Phys. Rev. Lett. **89**, 011301 (2002). Q. R. Ahmad *et al.* [SNO Collaboration], Phys. Rev. Lett. **89**, 011302 (2002).

[3] A. Bandyopadhyay, S. Choubey, S. Goswami and K. Kar, Phys. Lett. B **519**, 83 (2001).

[4] A. Bandyopadhyay, S. Choubey, S. Goswami and D. P. Roy, Phys. Lett. B **540**, 14 (2002); S. Choubey, A. Bandyopadhyay, S. Goswami and D. P. Roy, arXiv:hep-ph/0209222.

[5] G.L. Fogli, E. Lisi, D. Montanino, A. Palazzo, Phys. Rev. **D64**, 093007 (2001); J.N. Bahcall, M.C. Gonzalez-Garcia, C. Pana-Garay, JHEP **0108**, 014 (2001); P. I. Krastev and

A. Y. Smirnov, Phys. Rev. D **65**, 073022 (2002); M.V. Garzelli and C. Giunti, JHEP **0112**, 017 (2001).

[6] G. L. Fogli, E. Lisi, A. Marrone, D. Montanino and A. Palazzo, Phys. Rev. D **66**, 053010 (2002); J. N. Bahcall, M. C. Gonzalez-Garcia and C. Pena-Garay, JHEP **0207**, 054 (2002); V. Barger, D. Marfatia, K. Whisnant and B. P. Wood, Phys. Lett. B **537**, 179 (2002).

[7] K. Eguchi *et al.* [KamLAND Collaboration], Phys. Rev. Lett. **90**, 021802 (2003).

[8] A. Bandyopadhyay, S. Choubey, R. Gandhi, S. Goswami and D. P. Roy, Phys. Lett. B **559**, 121 (2003).

[9] G. L. Fogli et al., E. Lisi, A. Marrone, D. Montanino, A. Palazzo and A. M. Rotunno, Phys. Rev. D **67**, 073002 (2003); M. Maltoni, T. Schwetz and J. W. Valle, Phys. Rev. D **67**, 093003 (2003); J. N. Bahcall, M. C. Gonzalez-Garcia and C. Pena-Garay, JHEP **0302**, 009 (2003); H. Nunokawa, W. J. Teves and R. Zukanovich Funchal, Phys. Lett. B **562**, 28 (2003); P. Aliani, V. Antonelli, M. Picariello and E. Torrente-Lujan, Phys. Rev. D **69**, 013005 (2004);

P. C. de Holanda and A. Y. Smirnov, JCAP **0302**, 001 (2003).

[10] S. N. Ahmed *et al.* [SNO Collaboration], Phys. Rev. Lett. **92**, 181301 (2004).

[11] A. Bandyopadhyay, S. Choubey, S. Goswami, S. T. Petcov and D. P. Roy, Phys. Lett. B **583**, 134 (2004).

[12] G. L. Fogli, E. Lisi, A. Marrone and A. Palazzo, Phys. Lett. B **583**, 149 (2004); P. C. de Holanda and A. Y. Smirnov, Astropart. Phys. **21**, 287 (2004).

[13] T. Araki *et al.* [KamLAND Collaboration], Phys. Rev. Lett. **94**, 081801 (2005).

[14] A. Bandyopadhyay, S. Choubey, S. Goswami, S. T. Petcov and D. P. Roy, Phys. Lett. B **608**, 115 (2005).

[15] S. Goswami, A. Bandyopadhyay and S. Choubey, Nucl. Phys. Proc. Suppl. **143**, 121 (2005).

[16] . M. Maltoni, T. Schwetz, M. A. Tortola and J. W. F. Valle, New J. Phys. **6**, 122 (2004); G. L. Fogli, E. Lisi, A. Marrone and A. Palazzo, Prog. Part. Nucl. Phys. **57**, 742 (2006); J. N. Bahcall, M. C. Gonzalez-Garcia and C. Pena-Garay, JHEP **0408**, 016 (2004).

[17] M. Apollonio *et al.*, Eur. Phys. J. C **27**, 331 (2003).

[18] S. Abe *et al.* [KamLAND Collaboration], arXiv:0801.4589 [hep-ex].

[19] S. Goswami, Int. J. Mod. Phys. A **21**, 1901 (2006).

[20] S. Choubey, Phys. Atom. Nucl. **69**, 1930 (2006).

[21] Borexino Collaboration, Phys. Lett. B **658**, 101 (2008).

[22] A. Bandyopadhyay, S. Choubey and S. Goswami, Phys. Rev. D **67**, 113011 (2003).

[23] J. N. Bahcall and M. H. Pinsonneault, Phys. Rev. Lett. **92**, 121301 (2004).

[24] B. T. Cleveland *et al.*, Astrophys. J. **496**, 505 (1998).

[25] J. N. Abdurashitov *et al.* [SAGE Collaboration], J. Exp. Theor. Phys. **95**, 181 (2002) [Zh. Eksp. Teor. Fiz. **122**, 211 (2002)]; W. Hampel *et al.* [GALLEX Collaboration], Phys. Lett. B **447**, 127 (1999); C. Cattadori, Talk at Neutrino 2004, Paris, France, June 14-19, 2004.

[26] S. Fukuda *et al.* [Super-Kamiokande Collaboration], Phys. Lett. B **539**, 179 (2002).

[27] B. Aharmim *et al.* [SNO Collaboration], Phys. Rev. C **72**, 055502 (2005).

[28] L. Wolfenstein, Phys. Rev. D **17**, 2369 (1978) ; S. P. Mikheev and A. Y. Smirnov, Sov. J. Nucl. Phys. **42** (1985) 913 [Yad. Fiz. **42**, 1441 (1985)].

[29] A. Bandyopadhyay, S. Choubey, R. Gandhi, S. Goswami and D. P. Roy, J. Phys. G **29**, 2465 (2003).

[30] G.A. Horton-Smith, talk at Neutrino Oscillations in Venice, December 3-5, 2003, Venice, Italy; *http://axpd24.pd.infn.it/NO-VE/NO-VE.html*

[31] http : //www.fepc − atomic.jp/public¡nfo/public/index.html.

[32] Version 6 of the first reference of [16]; M. C. Gonzalez-Garcia and M. Maltoni, arXiv:0704.1800 [hep-ph]. A. B. Balantekin and D. Yilmaz, arXiv:0804.3345 [hep-ph].

[33] A. Bandyopadhyay, S. Choubey, S. Goswami and S. T. Petcov, Phys. Lett. B **581**, 62 (2004).

[34] S. Choubey and S. T. Petcov, Phys. Lett. B **594**, 333 (2004).

[35] A. Bandyopadhyay, S. Choubey, S. Goswami and S. T. Petcov, Phys. Rev. D **72**, 033013 (2005).

[36] H. Minakata, H. Nunokawa, W. J. C. Teves and R. Zukanovich Funchal, Phys. Rev. D **71**, 013005 (2005).

[37] S.T. Petcov, Phys. Lett. B **200**, 373 (1988), and Phys. Lett. B **214**, 139 (1988); S.T. Petcov and J. Rich, Phys. Lett. B **224**, 401 (1989); P.I. Krastev and S.T. Petcov, Phys. Lett. B **207**, 64 (1988); E. Lisi et al., Phys. Rev. D **63**, 093002 (2000).

[38] S.T. Petcov, Phys. Lett. B **214**, 259 (1988).

[39] S. Goswami and A. Y. Smirnov, Phys. Rev. D **72**, 053011 (2005).

[40] A. Bandyopadhyay, S. Choubey, S. Goswami and S. T. Petcov, Phys. Rev. D **75**, 093007 (2007).

[41] J. F. Beacom and M. R. Vagins, Phys. Rev. Lett. **93**, 171101 (2004).

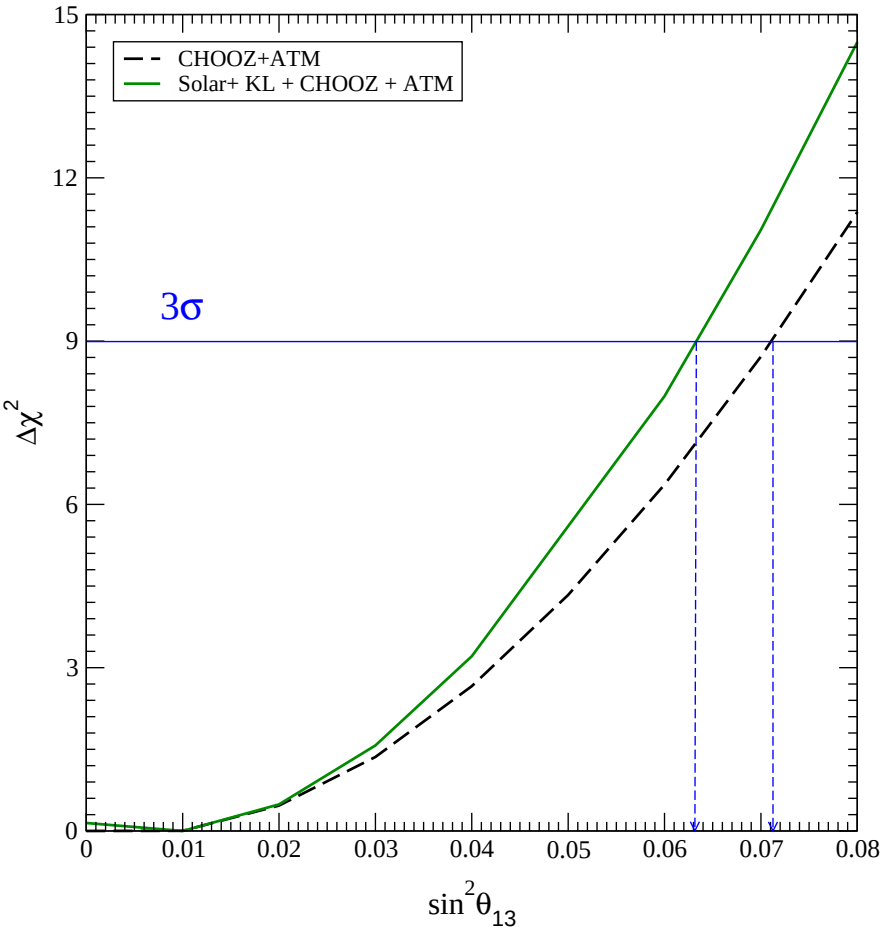

Figure 3: Bounds on the mixing angle θ_{13} using the CHOOZ data only (dashed line) and the combined solar, CHOOZ and KamLAND data (solid line). The Δm^2_{31} is allowed to vary freely in its current 3σ limit allowed by the atmospheric and long baseline neutrino data. The short-dashed verticle lines show the 3σ limits corresponding to the case of 1 parameter fit.

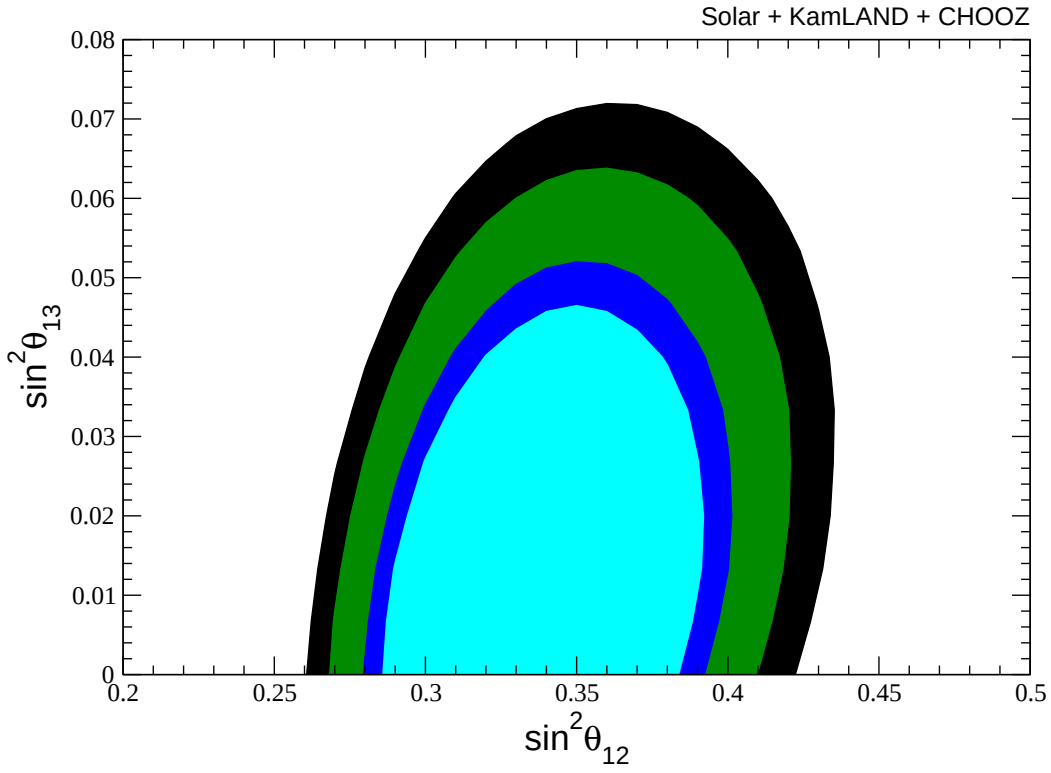

Figure 4: The 90%, 95%, 99% and 99.73% C.L. allowed regions in the $\sin^2\theta_{12} - \sin^2\theta_{13}$ plane, obtained in a three-neutrino oscillation analysis of the global solar and reactor neutrino data, including the data from the KamLAND and CHOOZ experiments. Here we use two parameter $\Delta\chi^2$ values to plot the C.L. contours.

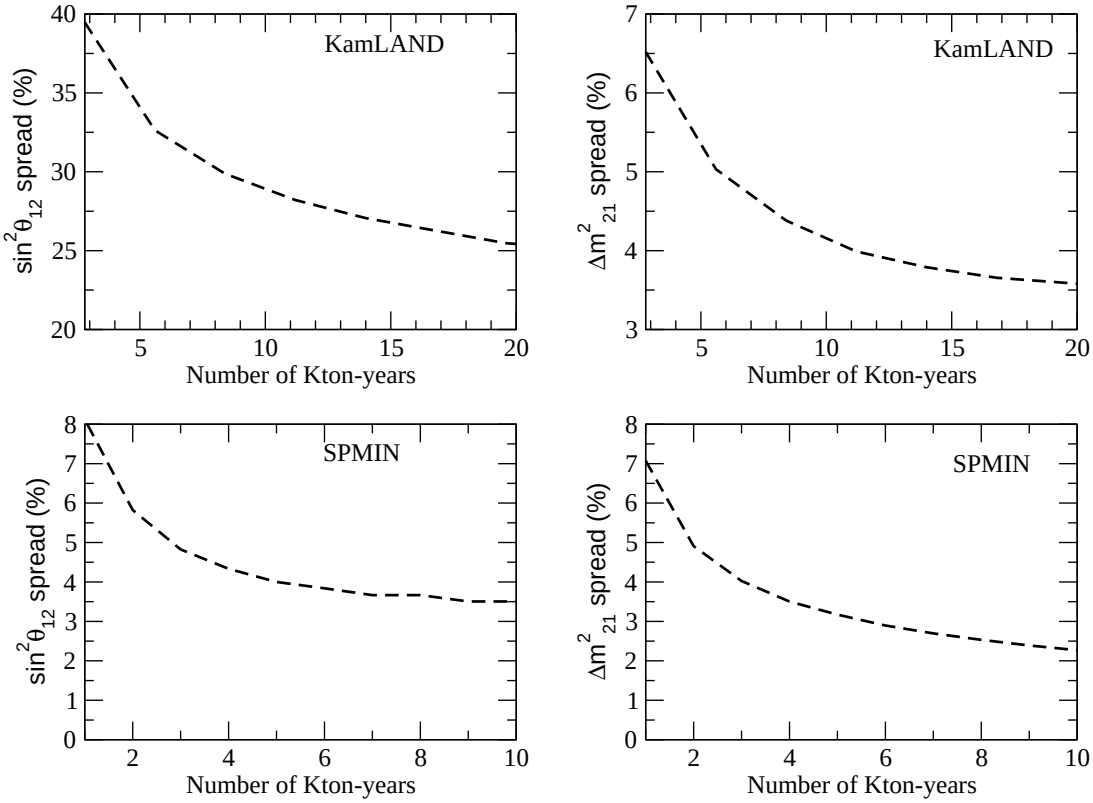

Figure 5: Expected 3σ spread of Δm^2_{21} and $\sin^2\theta_{12}$ as a function of the statistics for KamLAND (upper panels) and the SPMIN experiment (lower panels).